Two-point Random Gradient-free Methods for Model-free Feedback Optimization

Amir Mehrnoosh and Gianluca Bianchin

***Abstract*— Feedback optimization has emerged as a promising approach for optimizing the steady-state operation of dynamical systems while requiring minimal modeling efforts. Unfortunately, most existing feedback optimization methods rely on knowledge of the plant dynamics, which may be difficult to obtain or estimate in practice. In this paper, we introduce a novel randomized two-point gradient-free feedback optimization method, inspired by zeroth-order optimization techniques. Our method relies on function evaluations at two points to estimate the gradient and update the control input in real-time. We provide convergence guarantees and show that our method is capable of computing an ϵ-stationary point for smooth, nonconvex functions at a rate $\mathcal{O}(\epsilon^{-1})$, in line with existing results for two-point gradient-free methods for static optimization. Simulation results validate the findings.**

***Index Terms* – Model-free control, zeroth-order optimization, feedback optimization.**

I. Introduction

Feedback optimization (FO) is concerned with the problem of controlling dynamical systems to an optimal steady-state point, as characterized by a mathematical optimization problem [1]. Examples of the applicability of this framework include optimal scheduling in communication networks, resource scheduling in power grids, optimization of transportation systems, and operation of industrial control processes. Traditional numerical optimization methods [2] provide a systematic approach to make control decisions when an exact model of the plant to control is available, and led to a rich class of model-based FO methods [1], [3]–[8]. Yet, in real-world applications, an accurate model of the plant to control is rarely available [9], and thus implementing and ensuring the optimality of these methods remains challenging. To overcome these limitations, a model-free approach for FO has recently been proposed in [10], relying on a one-point residual-feedback gradient estimate [11]. Unfortunately, as is well-known in the optimization literature (see [11] for an insightful comparison), methods relying on one-point gradient estimates are unable to recover the rate of convergence of methods based on knowledge of the exact gradient [11]. Motivated by these limitations, in this paper, we propose a two-point random gradient-free method for feedback optimization. The proposed controller relies on two function evaluations of the plant performance to estimate a descent direction, combined with a random exploration step for the control input. To incorporate two function evaluations at each iteration, the controller is designed to operate at a slower timescale than that of the plant, in line with existing approaches on FO [5], [6], [8]. We show that, for smooth nonconvex problems, the proposed two-point method computes an ϵ-stationary point in $\mathcal{O}(\epsilon^{-1})$ iterations, this outperforms existing single-point methods [10], which are characterized by a rate of $\mathcal{O}(\epsilon^{-3/2})$ for the same problem.

Related works. Feedback optimization controllers have attracted significant interest due to their capacity to steer systems toward optimal steady states while effectively rejecting both constant and time-varying disturbances [5], [6], [8]. These approaches integrate numerical optimization into feedback control by leveraging real-time measurements to estimate gradients, thereby removing the reliance on accurate models of the plant and disturbances. In [12], a fast-stable plant is considered as an algebraic steady-state map for the power flow application. Particularly related to this work is the recent work [10], which is the first fully model-free method for feedback optimization, relying on a one-point residual-feedback gradient estimate [11].

Another key development in FO that emerged to address scalability and privacy issues in large-scale systems is distributed FO. When centralized approaches become impractical because of the system size or the need to keep internal states private, decentralized methods provide a viable alternative. Distributed gradient descent was first introduced in [13] and further analyzed in [14], with other distributed optimization algorithms extensively explored in [15]. Building on these foundations, the work [16] and [17] propose distributed FO methods that integrate FO with distributed computation to make FO practical for distributed architectures.

The literature on (static) zeroth-order optimization [18] is also related to this work. Zeroth-order methods refer to a class of optimization techniques that estimate gradients using function evaluations instead of explicit sensitivity information. These methods, such as one-point feedback [19] and an improved version [20], one-point residual feedback [11], and two-point feedback [21]–[24] include randomized gradient-free techniques. They have demonstrated convergence properties comparable to first-order approaches that make them suitable for model-free optimization. Specifically, two-point gradient-free methods that estimate gradients using finite differences between function evaluations at two distinct points are of particular interest because of their better rate of convergence relative to other gradient-free methods. However, this comes at the cost of increased computational complexity, as they require two function evaluations per estimation.

The authors are with ICTEAM Institute and the Department of Mathematical Engineering at UCLouvain, Belgium. A. Mehrnoosh is supported by F.R.S.-FNRS. {amir.mehrnoosh, gianluca.bianchin}@uclouvain.be.

Contributions. This work features two main contributions. First, we propose a two-point random gradient-free method for feedback optimization. In a net departure from [10], we utilize a two-point gradient estimate rather than a single-point one. Second, we provide a rigorous convergence analysis of our approach. Although our method requires two function evaluations to estimate a descent direction, its rate of convergence outperforms existing approaches based on a single evaluation. Importantly, our analysis shows that the rate of convergence of our method recovers that of established two-point gradient methods in static optimization [21].

Organization. The paper is structured as follows. Section II defines the problem focus of this work. Section III introduces the proposed two-point random gradient-free controller. Section IV presents the main theoretical results, followed by numerical validation in Section V. Finally, Section VI concludes the paper.

II. Problem formulation

We consider plants that can be modeled by a discrete-time dynamical models of the form:

$$\begin{aligned} x_{t+1} &= f(x_t, u_t, d), \\ y_t &= z(x_t, d), \end{aligned} \tag{1}$$

where $x_t \in \mathbb{R}^n$ is the system state at time t, $u_t \in \mathbb{R}^p$ the control input, $y_t \in \mathbb{R}^q$ the measured output, and $d \in \mathbb{R}^r$ models a deterministic but unknown constant disturbance. In this work, we are interested in an output regulation control problem; for this to be well-posed, we make the following assumption.

*Assumption 1 (**Properties of the plant**):* There exists a unique map $x_{\text{ss}} : \mathbb{R}^p \times \mathbb{R}^r \to \mathbb{R}^n$ such that $\forall u, d, f(x_{\text{ss}}(u,d), u, d) = x_{\text{ss}}(u,d)$; the mapping $u \mapsto x_{\text{ss}}(u,d)$ is globally M_x-Lipschitz in u, and the function $z(x,d)$ is globally M_z-Lipschitz in x. Moreover, for each (u,d), the equilibrium point $x_{\text{ss}}(u,d)$ of (1) is globally exponential stable; that is, there exists $\beta, \tau > 0$ such that for any $x_0 \in \mathbb{R}^n$, the solutions of (1) with $u_t = u \ \forall t$ satisfy $\|x_t - x_{\text{ss}}(u,d)\| \leq \beta \|x_0 - x_{\text{ss}}(u,d)\| e^{-\tau t}$. □

In other words, Assumption 1 guarantees the existence of a function x_{ss} that maps each input pair (u,d) into the corresponding equilibrium state and that the equilibrium of (1) is globally exponentially stable. We note that these assumptions are common in output regulation problems [25] as well as in feedback optimization approaches [5], [8], [17]. Notice also that if the plant to be regulated is not asymptotically stable, (1) shall be viewed as a pre-stabilized version of such a plant (e.g., stabilized via classical approaches based on output feedback [26]). In what follows, we let

$$h(u,d) \triangleq z(x_{\text{ss}}(u,d), d). \tag{2}$$

It follows from Assumption 1 that (1) is globally input-to-state stable with respect to the input $(u_{t+1} - u_t)$ (see [27]); that is, there exists[1] a $\mathcal{KL}$-function $\beta : \mathbb{R}_{\geq 0} \times \mathbb{R}_{\geq 0} \longrightarrow \mathbb{R}$ and a $\mathcal{K}$-function γ such that, for each input signal u_t and each $x_0 \in \mathbb{R}^n$, it holds that

$$\begin{aligned} \|x_{t+1} - x_{\text{ss}}(u_t, d)\| \leq \max_{1 \leq j \leq t} \{ &\sigma_1(\|x_1 - x_{\text{ss}}(u_0, d)\|), \\ &\sigma_2(\|u_j - u_{j-1}\|)\}, \end{aligned} \tag{3}$$

for all $x_1 \in \mathbb{R}^n$, where σ_1, σ_2 are two $\mathcal{K}$-functions. Motivated by this, we make the following assumption.

*Assumption 2 (**Properties of** $h(u,d)$):* There exists a $\mu \geq 0$ such that for any input $u_t \in \mathbb{R}^p$,

$$\|y_{t+1} - h(u_t, d)\|^2 \leq \mu.$$

□

The quantity μ can be interpreted as an estimate for the speed of the dynamics of the plant (1), capturing the rate at which (1) converges to its steady-state output. By comparison with (3), μ can be viewed as an estimate for the right-hand side of (3) (combined with the Lipschitz constant M_z). Notice that a uniform bound for the right-hand side of (3) is a reasonable approximation when $\|x_1 - x_{\text{ss}}(u_0, d)\|$ is bounded (in other words, the initial condition of (1) is close to the plant's steady-state), and the controller is sufficiently-slow, so that $\|u_j - u_{j-1}\|$ is bounded. We leave a relaxation of this assumption as the scope of future works.

In this work, we study the problem of designing a controller that regulates (1) to the solution of the following optimal output regulation problem:

$$\begin{aligned} \min_{u,y} \ & \Phi(u,y) \\ \text{s.t. } & y = h(u,d), \end{aligned} \tag{4}$$

where $\Phi : \mathbb{R}^p \times \mathbb{R}^q \to \mathbb{R}$ is a (possibly nonconvex) loss function modeling performance requirements for system inputs and outputs at steady-state. By substituting the constraint into the cost, (4) can be rewritten as an unconstrained optimization problem:

$$\min_u \ \tilde{\Phi}(u) \triangleq \Phi(u, h(u,d)). \tag{5}$$

We make the following assumption on the loss functions.

*Assumption 3 (**Properties of the optimization**):* The function $\tilde{\Phi}(u)$ is globally L-smooth, M-Lipschitz, and is bounded below by $\tilde{\Phi}_{\text{low}}$. Moreover, the function $\Phi(u,y)$ is globally M_Φ-Lipschitz in y. □

The assumptions on Lipschitz continuity in Assumption 3 are standard and largely satisfied in applications.

A standard approach to regulate (1) to the solution of (5) is as follows:

(S1) Apply an optimization algorithm to determine an optimizer $u^\star$ of (5)

(S2) Apply $u_t \equiv u^\star$ to (1)

Unfortunately, such an approach is impractical because of two main limitations:

(L1) Solving (5) requires knowledge of d, which in many practical applications is unknown

(L2) Solving (5) requires knowledge of the mapping $h(u,d)$ and hence of the full model of the plant (1) (precisely, of the functions $f(x,u,d)$, $z(x,d)$, and $x_{\text{ss}}(u,d)$

[1] See [27] for notation.

implicitly through (2)), which is impractical in many cases, as models are often unknown or inexact

Motivated by these observations, in this work we study the following problem.

Problem 1: Design a control algorithm for (1), having access only to performance evaluations of the plant at each time (i.e., oracle evaluations of $t \mapsto \Phi(u_t, y_{t+1})$) and without any knowledge of the disturbance d nor of the model of (1), such that the inputs and outputs of (1) converge asymptotically to an optimizer of (4). □

We stress that we seek an algorithm that relies on function evaluations of the map $\Phi(u, y)$ (cf. (4)) rather than $\tilde{\Phi}(u)$ (cf. (5)) because the mapping $h(u, d)$ is assumed to be unknown (see limitation(L2)), thus seeking a method that is entirely 'model-free.'

III. The two-point Random Gradient-free Method for Feedback Optimization

In this section, we propose a two-point random gradient-free method for feedback optimization that achieves the objectives set forward in Problem 1. The method is summarized in Algorithm 1. First, the input u_t is applied to the plant and the corresponding control performance is evaluated through $\Phi(u_t, y_{t+1})$ (cf. line 2). Then, the control input is randomly perturbed around the current point u_t (cf. line 3), applied to the plant, and the control performance is re-evaluated at such a perturbed point $\Phi(u_{t+1}, y_{t+2})$ (cf. line 4). By using these two function evaluations, a descent direction for the cost g_t^δ is estimated (cf. line 5) and, finally, the control decision is updated along this direction. In the algorithm, the parameter $\eta > 0$ is interpreted as the stepsize of the method and $\delta > 0$ as the smoothing parameter modeling the magnitude of the perturbation.

Algorithm 1: Two-point random gradient-free feedback controller

1: **Data:** $u_0 \in \mathbb{R}^p$, $x_0 \in \mathbb{R}^n$, $t = 0$, $\eta, \delta > 0$
2: Apply u_t to (1) and evaluate $\Phi(u_t, y_{t+1})$
3: Set $u_{t+1} = u_t + \delta v_t$, $v_t \sim \mathcal{N}(0, I_p)$
4: Apply u_{t+1} to (1) and evaluate $\Phi(u_{t+1}, y_{t+2})$
5: Set $g_t^\delta = \frac{v_t}{\delta}\big(\Phi(u_{t+1}, y_{t+2}) - \Phi(u_t, y_{t+1})\big)$
6: Set $u_{t+2} = u_t - \eta g_t^\delta$
7: $t \leftarrow t + 2$, go to step 2

Remark 1: Algorithm 1 can be seen as a variant of the random gradient-free two-point optimization method [21], [23], [28], specifically adapted for use in FO. This algorithm is characterized by two main innovative features with respect to [21], [23], [28]. First, each function evaluation $t \mapsto \Phi(u_t, y_{t+1})$ implicitly requires one state update of the plant (1) (namely, from x_t to x_{t+1}), and thus estimating a descent direction (as in line 5 of the algorithm) requires a combination of two plant updates. Moreover, because the algorithm relies on function evaluations of $\Phi(u, y)$ (in place of $\tilde{\Phi}(u)$) for the limitations outlined in (L1)-(L2), the descent direction estimated by g_t^δ is an *approximation* of a descent direction for $\tilde{\Phi}(u)$. These two properties pose additional challenges for the closed-loop performance analysis, which will be addressed in the subsequent sections. □

The closed-loop dynamics, when Algorithm 1 is used to control the plant (1) are, for[2] $t = 1, 2, 3, \dots$, given by:

$$x_{t+1} = f(x_t, u_t, d), \quad y_t = z(x_t, d), \tag{6}$$
$$u_{t+1} = \begin{cases} u_t + \delta v_t, \quad v_t \sim \mathcal{N}(0, I_p), & \text{if } t = 2, 4, 6, \dots, \\ u_{t-1} - \eta \frac{v_{t-1}}{\delta} g_{t-1}^\delta & \text{if } t = 1, 3, 5, \dots, \end{cases}$$

where $g_{t-1}^\delta = \big(\Phi(u_t, y_{t+1}) - \Phi(u_{t-1}, y_t)\big)$. The following result characterizes the control performance of Algorithm 1, when applied as a feedback controller as in (6).

Theorem 3.1: Suppose that Assumptions 1-3 hold. Fix $\epsilon_\Phi > 0$, and assume that $\eta < 1/8L(p+4)$ and $\delta \leq \sqrt{2\epsilon_\Phi/Lp}$. Then, the closed-loop system (6), after $T > 0$, iterations satisfies[3]:

$$\frac{1}{T}\sum_{k=0}^{T-1} E_v[\|\nabla\tilde{\Phi}(u_k)\|^2] = \mathcal{O}\left(\frac{1}{T\eta(1-\eta p)}\right) + \mathcal{O}\left(\frac{\eta\delta^2 p^3}{(1-\eta p)}\right) + \mathcal{O}\left(\delta^2 p^3\right) + \mathcal{O}\left(\frac{\mu p \eta}{\delta^2(1-\eta p)}\right), \tag{7}$$

where ϵ_Φ is the precision satisfying $|\tilde{\Phi}_\delta(u) - \tilde{\Phi}(u)| \leq \epsilon_\Phi$ and the expectation is with respect to $\{v_0, \dots, v_{T-1}\}$. □

The proof of this result is presented in Section IV. In other words, Theorem 3.1 guarantees that the control sequence u_k, produced by the closed-loop system (6), yields a sequence of gradient errors $\|\nabla\tilde{\Phi}(u_k)\|^2$ that is summable in expectation. The upper bound in (7) depends on the various parameters of the optimization problem (4), of the plant (1), and of the algorithm; in particular, the first term decreases to zero at a rate $1/T$, the second and third terms can be made arbitrarily small by carefully choosing a suitable small η and δ, while the fourth term depends on the rate of convergence of the plant and can be reduced when μ is a tunable parameter. In fact, for a rapidly decaying system (μ close to zero), this term can be neglected.

Remark 2: In Theorem 3.1, the average second moment of the gradient of the $\tilde{\Phi}(u)$ is the convergence measure. This measure is extensively used in the field of zeroth-order optimization when the problem is nonconvex [11], [21]. We say a solution u is ϵ-accurate if $E[\|\nabla\tilde{\Phi}(u)\|^2] \leq \epsilon$. Note that finding a globally optimal solution for nonconvex problems is NP-hard [29]. Hence, this measure serves as a starting point for analysis in this work. In addition, we need the Gaussian smooth approximation $\tilde{\Phi}_\delta$ to be ϵ_Φ-close to the original objective function $\tilde{\Phi}$, which requires $\delta \leq \sqrt{2\epsilon_\Phi/Lp}$ according to Lemma 1.1 in the Appendix.

□

The following result gives an explicit way to select all parameters of the optimization method to ensure that the iterates of (6) converge to an ϵ-stationary point of (5).

[2] See the detailed description in Algorithm 1 for initializations and the special case $t = 0$.

[3] A function $\psi(n)$ is said to be $\mathcal{O}\big(f(n)\big)$ if there exists a constant $C > 0$ and n_0 such that $\forall n \geq n_0$, $|\psi(n)| \leq C|f(n)|$.

Theorem 3.2: Suppose that Assumptions 1-3 hold. Fix $\epsilon, \epsilon_\Phi > 0$, let $\eta = 1/16L(p+4)$,

$$\delta^2 = \sqrt{\frac{4M_\Phi^2 \mu p(8p+33)}{L^2(p+4)\big((p+6)^3+(p+4)^2\big)}}, \tag{8}$$

and suppose that $\mu \leq \min\{\mu_1, \mu_2\}$, where

$$\mu_1 = \frac{(p+4)\epsilon^2}{16L^2M_\Phi^2 p(8p+33)\big((p+6)^3+(p+4)^2\big)},$$
$$\mu_2 = \frac{(p+4)\big((p+6)^3+(p+4)^2\big)\epsilon_\Phi^2}{M_\Phi^2 p^3(8p+33)}. \tag{9}$$

Then, after $T \geq 2c_1/\epsilon$ iterations, the closed-loop system (6) satisfies:

$$\frac{1}{T}\sum_{k=0}^{T-1} E_v[\|\nabla\tilde{\Phi}(u_k)\|^2] \leq \epsilon, \tag{10}$$

where $c_1 = 128L(p+4)(\tilde{\Phi}_\delta(u_0) - \tilde{\Phi}_{low})$ and the expectation is taken with respect to $\{v_0, \ldots, v_{T-1}\}$.

The proof of this result is presented in Section IV. In other words, given a desired accuracy ϵ, Theorem 3.2 gives a method to select the parameters η and δ so that (6) reaches an ϵ-stationary point of (5). Notice the choice of η and δ made here are compatible with the range for these parameters given in Theorem 3.1. Particularly, by combining (8) with (9), it follows that, to reach an ϵ-stationary point, the smoothing parameter should be chosen $\delta^2 = \mathcal{O}(\frac{\max\{\epsilon,\epsilon_\Phi\}}{L^2p^3})$.

Remark 3: Interestingly, the required iteration complexity for the proposed algorithm is of order $\mathcal{O}(p\epsilon^{-1})$, which is the same as the best complexity result for two-point zeroth-order feedback established in [21], whereas the iteration complexity for the one-point residual feedback is of order $\mathcal{O}(p^3\epsilon^{-3/2})$. Note that this comparison holds when the objective function is smooth and nonconvex [11]. □

IV. Convergence and Performance Analysis

In this section, we analyze the iterates of (6) and present the proofs of Theorems 3.1-3.2.

First, we introduce the compact notation:

$$\tilde{g}_\delta(u_t) := \frac{v_t}{\delta}\big(\tilde{\Phi}(u_t+\delta v_t) - \tilde{\Phi}(u_t)\big),$$
$$g_\delta(u_t) := \frac{v_t}{\delta}\big(\Phi(u_{t+1}, y_{t+2}) - \Phi(u_t, y_{t+1})\big), \tag{11}$$

and observe that $\tilde{g}_\delta(u_t)$ models the two-point gradient estimator [21], [23], [28] based for the true function $\tilde{\Phi}(u_k)$ that we aim to minimize (see (5)). Moreover, define the gradient estimator error:

$$e_t := g_\delta(u_t) - \tilde{g}_\delta(u_t). \tag{12}$$

A. Instrumental results

The following results are instrumental for the subsequent analysis.

Lemma 4.1 ([21, Lemma 1]): Let $v \in \mathbb{R}^p$ satisfy the standard multivariate normal distribution. Then,

$$E[\|v\|^t] \leq \begin{cases} p^{t/2}, & \text{if } t \in [0,2], \\ (p+t)^{t/2}, & \text{if } t > 2. \end{cases}$$

□

Lemma 4.2: If Assumptions 1-3 hold, then

$$E[\|e_t\|^2] \leq \frac{4M_\Phi^2\mu p}{\delta^2}. \tag{13}$$

□

Proof: By substituting (11) into (12):

$$e_t = \frac{v_t}{\delta}\big[\Phi(u_{t+1}, y_{t+2}) - \Phi(u_t, y_{t+1}) - \big(\tilde{\Phi}(u_{t+1}) - \tilde{\Phi}(u_t)\big)\big]. \tag{14}$$

Now, we take the 2-norm from both sides of the inequality and use $(a+b)^2 \leq 2a^2 + 2b^2$. Noting that $\tilde{\Phi}(u_t) = \Phi(u_t, h(u_t, d))$, we obtain

$$\begin{aligned}\|e_t\|^2 &\leq \frac{2\|v_t\|^2}{\delta^2}\big\|\Phi(u_{t+1}, y_{t+2}) - \Phi(u_{t+1}, h(u_{t+1}, d))\big\|^2 \\ &\quad + \frac{2\|v_t\|^2}{\delta^2}\big\|\Phi(u_t, y_{t+1}) - \Phi(u_t, h(u_t, d))\big\|^2, \\ &\overset{(a)}{\leq} \frac{2\|v_t\|^2}{\delta^2}M_\Phi^2\big(\|y_{t+2} - h(u_{t+1}, d)\|^2 \\ &\qquad + \|y_{t+1} - h(u_t, d)\|^2\big), \\ &\overset{(b)}{\leq} \frac{4\|v_t\|^2}{\delta^2}M_\Phi^2\mu,\end{aligned} \tag{15}$$

where (a) follows from the Lipschitz continuity of $\Phi(u, y)$ in y, and (b) from Assumption 2. Taking the expectations of both sides of 15, and utilizing Lemma 4.1 completes the proof. ■

Let $\{a_k\}_{k=0}^\infty, a_k = 2k$, denote the sequence of even, non-negative, integers. With a slight abuse of notation, in what follows, we will denote a_k simply by k, such that $k+1$ is intended to denote $a_{k+1} = 2(k+1)$. Notice also that we will use the notation k to explicitly distinguish it from the time index t in (6).

B. Proof of Theorems 3.1-3.2

We begin with the proof of Theorem 3.1. From Assumption 3, we have

$$\begin{aligned}&\tilde{\Phi}_\delta(u_{k+1}) \\ &\leq \tilde{\Phi}_\delta(u_k) + \big\langle\nabla\tilde{\Phi}_\delta(u_k), u_{k+1} - u_k\big\rangle + \frac{L}{2}\|u_{k+1} - u_k\|^2 \\ &\overset{(a)}{\leq} \tilde{\Phi}_\delta(u_k) - \eta\big\langle\nabla\tilde{\Phi}_\delta(u_k), \tilde{g}_\delta(u_k) + e_k\big\rangle \\ &+ \frac{L\eta^2}{2}\|\tilde{g}_\delta(u_k) + e_k\|^2,\end{aligned} \tag{16}$$

where (a) follows from line 5 of Algorithm 1 and (12). By taking the expectations of both sides of (16) with respect to v_k and using $(a+b)^2 \leq 2a^2 + 2b^2$ inequality on the third

term, we have

$$
\begin{aligned}
&E_{v_k}[\tilde{\Phi}_\delta(u_{k+1})] \\
&\quad\le \tilde{\Phi}_\delta(u_k) - \eta\big\langle\nabla\tilde{\Phi}_\delta(u_k), E_{v_k}[\tilde{g}_\delta(u_k)]\big\rangle \\
&\quad- \eta\big\langle\nabla\tilde{\Phi}_\delta(u_k), E_{v_k}[e_k]\big\rangle + L\eta^2 E_{v_k}\big[\|\tilde{g}_\delta(u_k)\|^2\big] \\
&\quad+ L\eta^2 E_{v_k}\big[\|e_k\|^2\big] \\
&\quad\overset{(a)}{\le} \tilde{\Phi}_\delta(u_k) - \eta\|\nabla\tilde{\Phi}_\delta(u_k)\|^2 - \eta\big\langle\nabla\tilde{\Phi}_\delta(u_k), E_{v_k}[e_k]\big\rangle \\
&\quad+ L\eta^2 E_{v_k}\big[\|\tilde{g}_\delta(u_k)\|^2\big] + L\eta^2 E_{v_k}\big[\|e_k\|^2\big] \\
&\quad\overset{(b)}{\le} \tilde{\Phi}_\delta(u_k) - \eta\|\nabla\tilde{\Phi}_\delta(u_k)\|^2 - \eta\big\langle\nabla\tilde{\Phi}_\delta(u_k), E_{v_k}[e_k]\big\rangle \\
&\quad+ 4L\eta^2(p+4)\|\nabla\tilde{\Phi}_\delta(u_k)\|^2 + 3L^3\eta^2\delta^2(p+4)^3 \\
&\quad+ L\eta^2 E_{v_k}\big[\|e_k\|^2\big] \qquad (17)
\end{aligned}
$$

where (a) and (b) follow from Lemma 1.2(i) and (ii) in Appendix, respectively. By rearranging terms, we obtain

$$
\begin{aligned}
&\big(\eta - 4L\eta^2(p+4)\big)\|\nabla\tilde{\Phi}_\delta(u_k)\|^2 \\
&\le \tilde{\Phi}_\delta(u_k) - E_{v_k}[\tilde{\Phi}_\delta(u_{k+1})] - \eta\big\langle\nabla\tilde{\Phi}_\delta(u_k), E_{v_k}[e_k]\big\rangle \\
&+ 3L^3\eta^2\delta^2(p+4)^3 + L\eta^2 E_{v_k}\big[\|e_k\|^2\big] \\
&\overset{(a)}{\le} \tilde{\Phi}_\delta(u_k) - E_{v_k}[\tilde{\Phi}_\delta(u_{k+1})] + \frac{\eta}{2}\|\nabla\tilde{\Phi}_\delta(u_k)\|^2 \\
&+ \frac{\eta}{2}\|E_{v_k}[e_k]\|^2 + 3L^3\eta^2\delta^2(p+4)^3 + L\eta^2 E_{v_k}\big[\|e_k\|^2\big] \qquad (18)
\end{aligned}
$$

where (a) follows from $< a, b > \le \|a\|\|b\| \le \frac{1}{2}(\|a\|^2 + \|b\|^2)$. Exploiting Jensen's inequality, we have

$$
\begin{aligned}
&\big(\frac{\eta}{2} - 4L\eta^2(p+4)\big)\|\nabla\tilde{\Phi}_\delta(u_k)\|^2 \\
&\le \tilde{\Phi}_\delta(u_k) - E_{v_k}[\tilde{\Phi}_\delta(u_{k+1})] + 3L^3\eta^2\delta^2(p+4)^3 \\
&+ (L\eta^2 + \frac{\eta}{2})E_{v_k}\big[\|e_k\|^2\big]. \qquad (19)
\end{aligned}
$$

Note that the left-hand side of (19) is positive ($0 < \eta < 1/8L(p+4)$). Now, we define $\xi := \big(\eta/2 - 4L\eta^2(p+4)\big)$. Combining (19) and Lemma 1.1(ii), we have

$$
\begin{aligned}
&\|\nabla\tilde{\Phi}(u_k)\|^2 \\
&\le \frac{2}{\xi}\big(\tilde{\Phi}_\delta(u_k) - E_{v_k}[\tilde{\Phi}_\delta(u_{k+1})]\big) + \frac{6}{\xi}L^3\eta^2\delta^2(p+4)^3 \\
&+ \frac{1}{\xi}(2L\eta^2 + \eta)E_{v_k}\big[\|e_k\|^2\big] + \frac{1}{2}\delta^2L^2(p+6)^3. \qquad (20)
\end{aligned}
$$

Taking the expectations of both sides of (20) with respect to $v_0, \ldots, v_{k-1}$, we have

$$
\begin{aligned}
&E\big[\|\nabla\tilde{\Phi}(u_k)\|^2\big] \\
&\le \frac{2}{\xi}\big(E[\tilde{\Phi}_\delta(u_k)] - E[\tilde{\Phi}_\delta(u_{k+1})]\big) + \frac{6}{\xi}L^3\eta^2\delta^2(p+4)^3 \\
&+ \frac{1}{\xi}(2L\eta^2 + \eta)E\big[\|e_k\|^2\big] + \frac{1}{2}\delta^2L^2(p+6)^3. \qquad (21)
\end{aligned}
$$

Summing up from $k = 0, \ldots, T-1$, we obtain

$$
\begin{aligned}
&\sum_{k=0}^{T-1} E_v[\|\nabla\tilde{\Phi}(u_k)\|^2] \\
&\le \frac{2}{\xi}\big(E[\tilde{\Phi}_\delta(u_0)] - E[\tilde{\Phi}_\delta(u_T)]\big) + \frac{6}{\xi}TL^3\eta^2\delta^2(p+4)^3 \\
&+ \frac{1}{\xi}(2L\eta^2 + \eta)\sum_{k=0}^{T-1} E\big[\|e_k\|^2\big] + \frac{1}{2}T\delta^2L^2(p+6)^3 \\
&\overset{(a)}{\le} \frac{2}{\xi}\big(\tilde{\Phi}_\delta(u_0) - \tilde{\Phi}_{low}\big) + \frac{6}{\xi}TL^3\eta^2\delta^2(p+4)^3 \\
&+ \frac{1}{\xi}(2L\eta^2 + \eta)\sum_{k=0}^{T-1} E\big[\|e_k\|^2\big] + \frac{1}{2}T\delta^2L^2(p+6)^3, \\
&\overset{(b)}{\le} \frac{2}{\xi}\big(\tilde{\Phi}_\delta(u_0) - \tilde{\Phi}_{low}\big) + \frac{6}{\xi}TL^3\eta^2\delta^2(p+4)^3 \\
&+ \frac{4M_\Phi^2\mu pT}{\xi\delta^2}(2L\eta^2 + \eta) + \frac{1}{2}T\delta^2L^2(p+6)^3, \qquad (22)
\end{aligned}
$$

where (a) follows the fact that $\tilde{\Phi}$ is bounded from below, and (b) obtained from Lemma 4.2. Finally, we divide the both sides of (22) by T, and substitute ξ, which lead to

$$
\begin{aligned}
&\frac{1}{T}\sum_{k=0}^{T-1} E_v[\|\nabla\tilde{\Phi}(u_k)\|^2] \\
&\le \frac{4\big(\tilde{\Phi}_\delta(u_0) - \tilde{\Phi}_{low}\big)}{T\eta\big(1 - 8L\eta(p+4)\big)} + \frac{12L^3\eta\delta^2(p+4)^3}{1 - 8L\eta(p+4)} \\
&+ \frac{8M_\Phi^2\mu p(2L\eta+1)}{\delta^2\big(1 - 8L\eta(p+4)\big)} + \frac{\delta^2L^2(p+6)^3}{2} \\
&\le \mathcal{O}\bigg(\frac{1}{T\eta(1-\eta p)}\bigg) + \mathcal{O}\bigg(\frac{\eta\delta^2p^3}{(1-\eta p)}\bigg) + \mathcal{O}\bigg(\frac{\mu p\eta}{\delta^2(1-\eta p)}\bigg) \\
&+ \mathcal{O}\Big(\delta^2p^3\Big). \qquad (23)
\end{aligned}
$$

Completing the proof of Theorem 3.1, we continue to prove Theorem 3.2. First, we set $\eta = 1/16L(p+4)$ and substitute it in (23). We obtain

$$
\frac{1}{T}\sum_{k=0}^{T-1} E_v[\|\nabla\tilde{\Phi}(u_k)\|^2] \le \frac{c_1}{T} + \frac{c_2L^2\delta^2}{2} + \frac{c_3\mu}{\delta^2}, \qquad (24)
$$

where

$$
\begin{aligned}
c_2 &= (p+6)^3 + (p+4)^2, \\
c_3 &= \frac{2M_\Phi^2p(8p+33)}{p+4}.
\end{aligned}
$$

Then, we minimize the right-hand side of (24) with respect to δ. Substituting δ with its optimal value, as given in the theorem statement, we get

$$
\frac{1}{T}\sum_{k=0}^{T-1} E_v[\|\nabla\tilde{\Phi}(u_k)\|^2] \le \frac{c_1}{T} + L\sqrt{2c_2c_3\mu} \le \epsilon. \qquad (25)
$$

Solving $c_1/T \le \epsilon/2$ for T and $L\sqrt{2c_2c_3\mu} \le \epsilon/2$ for μ give the lower bound for the number of iterations required to reach

ϵ-accuracy convergence and μ_1, respectively. Furthermore, from Lemma 1.1(ii),

$$|\tilde{\Phi}_\delta(u) - \tilde{\Phi}(u)| \leq \frac{\delta^2}{2} Lp = \frac{p\sqrt{c_3\mu}}{\sqrt{2c_2}} \leq \epsilon_\Phi. \tag{26}$$

Solving (26) for μ gives μ_2 and completes the proof.

V. Simulation Results

In this section, we show the performance of the proposed Algorithm 1. In line with [10], we consider the following nonlinear system:

$$\begin{aligned} x_{t+1} &= Ax_t + Bu_t + Ed_x \\ &\quad + F\big(x_t - x_{\text{ss}}(u_t, d_x)\big) \otimes \big(x_t - x_{\text{ss}}(u_t, d_x)\big) \\ y_t &= Cx_t + Dd_y, \end{aligned} \tag{27}$$

where $x \in \mathbb{R}^{10}$, $u \in \mathbb{R}^5$, $d_x, d_y \in \mathbb{R}^5$ and $y \in \mathbb{R}^5$ are the state, input, disturbances, and output of the system, accordingly. Moreover, $x_{\text{ss}}(u_t, d_x) \triangleq (I-A)^{-1}(Bu_t + Ed_x)$ is the steady-state map, where I is the identity matrix of the corresponding order. The final term in the state equation of (27) can be interpreted as the residual error when linear dynamics serve as an approximation for general nonlinear dynamics at steady state. The system matrices in (27) are randomly drawn from the standard uniform distribution. Also, we let $\|A\|_2 = 0.05$ and $\|F\|_1 = 0.01$ to ensure the stability of the system. The disturbances d_x, d_y are produced from the standard normal distribution. We consider the following instance of (4):

$$\min_{u,y} \ \Phi(u, y) = u^\top R_1 u + R_2^\top u + \|y\|^2. \tag{28}$$

In (28), we define the positive semi-definite matrix $R_1 = R_3^\top R_3 \in \mathbb{R}^{5\times5}$. The elements of $R_2 \in \mathbb{R}^5$ and $R_3 \in \mathbb{R}^{5\times5}$ are drawn from the standard uniform distribution. Thus, the objective in (28) is a smooth convex function.

In Fig. 1, we propose a comparison between the performance of Algorithm 1, the FO method with exact gradient [9], an idealized two-point method where the state of the plant is restarted at each iteration mimicking [21], [23], [28], and the one-point residual feedback optimization [10]. More precisely, the FO method with exact gradient [9] is given by:

$$u_{t+1} = u_t - \eta\big(\nabla_u \Phi(u_t, y_{t+1}) + G^\top \nabla_y \Phi(u_t, y_{t+1})\big), \tag{29}$$

where $G \triangleq C(I-A)^{-1}B$ is the steady-state input to output sensitivity of (27) and $\eta > 0$ is the stepsize.

In Fig. 1, we compare the performance of the different methods using the squared norm of the gradient of the objective $\tilde{\Phi}(u_t)$ and the optimality gap $\tilde{\Phi}(u_t) - \tilde{\Phi}_{\text{low}}$, where $\tilde{\Phi}_{\text{low}}$ is the minimizer of the problem (28). To obtain this figure, we used $\delta = 5 \times 10^{-5}$; the selected stepsizes are 40×10^{-5}, 2.5×10^{-5}, and 100×10^{-5} for the modified and idealized two-point FO controller, the one-point residual FO controller, and the first-order controller (29) with the exact gradient of the objective, respectively. The selected stepsizes have been optimized via trial-and-error, selecting the largest

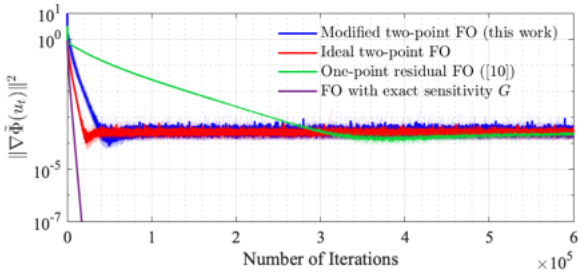

(a) Comparison of the squared norm of the cost gradient for each method.

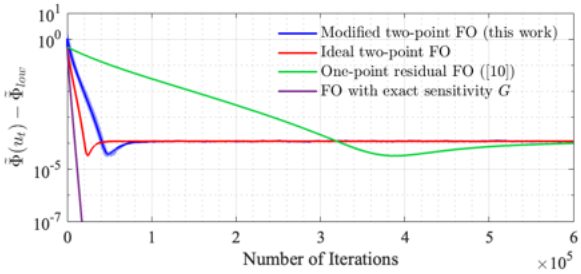

(b) Comparison of the optimality gap for each method.

Fig. 1. Comparison of the proposed modified two-point FO ($\eta = 40\times10^{-5}$), idealized two-point FO ($\eta = 40\times10^{-5}$), one-point residual proposed in [10] ($\eta = 2.5\times10^{-5}$), and classical first-order gradient descent with the exact gradient of the cost ($\eta = 100\times10^{-5}$). δ is set to 5×10^{-5} for all methods.

values that yield a converging algorithm. In the figures, the solid curve represents the average trajectory across 10 experiments, whereas the shaded region illustrates the variation in these trajectories. We note that all randomized methods yield moderate oscillatory trajectories, arising from the stochastic nature of input perturbations. In contrast, the exact method (29) does not exhibit this behavior because of its deterministic nature.

In Fig. 1(a), we observe that the feedback controller using the exact sensitivity G outperforms the others; Algorithm 1 gives a solution accuracy and a convergence rate comparable to the idealized two-point but converges more slowly; the one-point residual feedback methods [10] has a rate a convergence that is considerably worse than all other methods considered. This aligns with the existing theoretical guarantees, which shows that random two-point gradient-free methods generally exhibit faster convergence than random one-point gradient-free methods [11]. A similar pattern is observed in Fig. 1(b); the first-order controller achieves the best performance, and the proposed modified controller convergence rate is close to that of the idealized two-point controller and surpasses the one-point residual controller. Moreover, the feedback mechanism of these controllers inherently reduces spikes caused by disturbances.

Fig. 2 illustrates the impact of the stepsize (η) and the smoothing parameter (δ). Decreasing the smoothing ratio δ, in general, leads to an improvement in steady-state accuracy and reduces high-frequency variations due to large exploration steps (cf. Fig. 2 blue line and red line). However, in our simulations, we observed that exceedingly small values of δ may lead to algorithms with poor robustness when noise

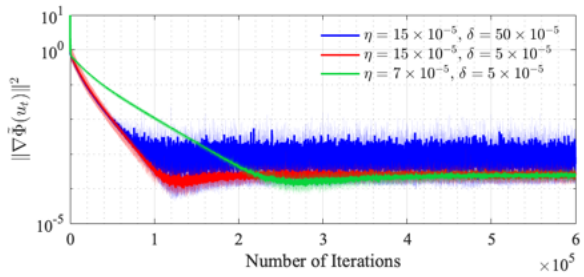

Fig. 2. Performance of the proposed modified two-point FO for different stepsize (η) and smoothing parameter (δ).

is involved in the sensing and actuation signals, as noise may interfere with the exploration step (step 2 of Algorithm 1). On the other hand, increasing the stepsize (η) within the allowable range improves the rate of convergence (cf. Fig. 2 green line and red line).

VI. Conclusions

This paper introduced a two-point gradient-free feedback optimization method for controlling dynamical systems to an optimal steady-state point. Unlike traditional FO methods that rely on model-dependent gradient estimates, the proposed algorithm estimates the gradient using function evaluations, which makes it fully model-free. We modified the standard two-point zeroth-order method to make it practical for control systems. Theoretical analysis provided guarantees on the convergence of the method, and we compared the proposed algorithm with other existing zeroth-order algorithms to show its effectiveness. Further studies could extend the algorithm to a constrained optimization problem and explore adaptive stepsize to enhance the performance. In addition, relaxing the assumption on contraction properties would be an interesting research direction.

Appendix

A. Zeroth-Order Optimization

Zeroth-order or gradient-free optimization is the concept of utilizing function evaluations to estimate the gradient of the cost without the need to access the gradient directly. Zeroth-order optimization is a well-studied field; as such, the seminal work of [21] sets a concrete framework in this field, introducing two-point gradient estimates, which we utilize in this work. The goal is to approximate the first-order gradient of a function using only function evaluations. To achieve this, we need to perturb the function around the current point in a uniformly distributed manner across all directions that leads to considering a Gaussian-smoothed version of the function $f(u) : \mathbb{R}^p \to \mathbb{R}$, as introduced by [21],

$$f_\delta(u) := E_{v\sim\mathcal{N}(0,I_p)}[f(u+\delta v)], \tag{30}$$

where the elements of the vector v are i.i.d. standard Gaussian random variables. The following Lemma bounds the approximation error of the function $f_\delta(u)$, which is developed in [21].

Lemma 1.1 ([21, Theorem 1 and Lemma 4]): If $f : \mathbb{R}^p \to \mathbb{R}$ is L-smooth, then for any $u \in \mathbb{R}^p$, $\delta > 0$, and $f_\delta(u)$ given in (30),

$$(i) \quad |f_\delta(u) - f(u)| \le \frac{\delta^2}{2} Lp,$$
$$(ii) \quad \|\nabla f(u)\|^2 \le 2\|\nabla f_\delta(u)\|^2 + \frac{\delta^2}{2} L^2 (p+6)^3.$$

□

For an objective function $f(u) : \mathbb{R}^p \to \mathbb{R}$, the gradient-free oracle proposed in [21] is

$$\tilde{g}_\delta(u_t) = \frac{v_t}{\delta}\big(f(u_t + \delta v_t) - f(u_t)\big) \tag{31}$$

where v_t is a random vector of the corresponding size drawn from the standard multivariate normal distribution, and δ is a smoothing parameter, which represents the amplitude of the exploration noise. Note that the gradient estimation in (31) requires two function evaluations at time t, which poses a challenge in the control setting, as only one actuation step can be applied to the system at a given time. In this work, we modify the algorithm to make it compatible with the FO setting.

Lemma 1.2 ([21, Lemma 5]): If $f : \mathbb{R}^p \to \mathbb{R}$ is L-smooth, given any $u \in \mathbb{R}^p$, $\delta > 0$, $v \sim \mathcal{N}(0, I_p)$, $f_\delta(u)$ in (30), and $\tilde{g}_\delta(u)$ in (31),

$$(i) \quad E_v[\tilde{g}_\delta(u)] = \nabla f_\delta(u),$$
$$(ii) \quad E_v[\|\tilde{g}_\delta(u)\|^2] \le 4(p+4)\|\nabla f_\delta(u)\|^2 + 3\delta^2 L^2 (p+4)^3.$$

□

Lemma 1.2 shows that the estimator (31) is an unbiased gradient estimate of the smoothed function $f_\delta(u)$ at u_t besides a bound on the second moment of the gradient estimate $E_v[\|\tilde{g}_\delta(u)\|^2]$, which is used in our analysis in Section IV.

References

[1] A. Jokic, M. Lazar, and P. van den Bosch, "On constrained steady-state regulation: Dynamic KKT controllers," *IEEE Transactions on Automatic Control*, vol. 54, no. 9, pp. 2250–2254, 2009.

[2] Y. Nesterov *et al.*, *Lectures on convex optimization*. Springer, 2018, vol. 137.

[3] F. Brunner, H.-B. Dürr, and C. Ebenbauer, "Feedback design for multi-agent systems: A saddle point approach," in *IEEE Conf. on Decision and Control*, 2012, pp. 3783–3789.

[4] M. Colombino, E. Dall'Anese, and A. Bernstein, "Online optimization as a feedback controller: Stability and tracking," *IEEE Transactions on Control of Network Systems*, vol. 7, no. 1, pp. 422–432, 2020.

[5] G. Bianchin, J. Cortés, J. I. Poveda, and E. Dall'Anese, "Time-varying optimization of LTI systems via projected primal-dual gradient flows," *IEEE Transactions on Control of Network Systems*, vol. 9, no. 1, pp. 474–486, Mar. 2022.

[6] G. Bianchin, J. I. Poveda, and E. Dall'Anese, "Online optimization of switched LTI systems using continuous-time and hybrid accelerated gradient flows," *Automatica*, vol. 146, p. 110579, Aug. 2022.

[7] G. Belgioioso, D. Liao-McPherson, M. H. de Badyn, S. Bolognani, J. Lygeros, and F. Dörfler, "Sampled-data online feedback equilibrium seeking: Stability and tracking," in *IEEE Conf. on Decision and Control*, 2021, pp. 2702–2708.

[8] A. Hauswirth, S. Bolognani, G. Hug, and F. Dörfler, "Timescale separation in autonomous optimization," *IEEE Transactions on Automatic Control*, vol. 66, no. 2, pp. 611–624, 2021.

[9] G. Bianchin, M. Vaquero, J. Cortes, and E. Dall'Anese, "Online stochastic optimization for unknown linear systems: Data-driven controller synthesis and analysis," *IEEE Transactions on Automatic Control*, vol. 69, no. 7, pp. 4411–4426, 2023.

[10] Z. He, S. Bolognani, J. He, F. Dörfler, and X. Guan, "Model-free nonlinear feedback optimization," *IEEE Transactions on Automatic Control*, vol. 69, no. 7, pp. 4554–4569, 2023.

[11] Y. Zhang, Y. Zhou, K. Ji, and M. M. Zavlanos, "A new one-point residual-feedback oracle for black-box learning and control," *Automatica*, vol. 136, p. 110006, 2022.

[12] Y. Chen, A. Bernstein, A. Devraj, and S. Meyn, "Model-free primal-dual methods for network optimization with application to real-time optimal power flow," in *2020 American Control Conference (ACC)*. IEEE, 2020, pp. 3140–3147.

[13] A. Nedic and A. Ozdaglar, "Distributed subgradient methods for multi-agent optimization," *IEEE Transactions on Automatic Control*, vol. 54, no. 1, pp. 48–61, 2009.

[14] K. Yuan, Q. Ling, and W. Yin, "On the convergence of decentralized gradient descent," *SIAM Journal on Optimization*, vol. 26, no. 3, pp. 1835–1854, 2016.

[15] T. Yang, X. Yi, J. Wu, Y. Yuan, D. Wu, Z. Meng, Y. Hong, H. Wang, Z. Lin, and K. H. Johansson, "A survey of distributed optimization," *Annual Reviews in Control*, vol. 47, pp. 278–305, 2019.

[16] A. Mehrnoosh and G. Bianchin, "Distributed optimization of linear multi-agent systems via feedback-dgd," *arXiv preprint arXiv:2403.18386*, 2024, to appear on the American Control Conference 2025.

[17] G. Carnevale, N. Mimmo, and G. Notarstefano, "Nonconvex distributed feedback optimization for aggregative cooperative robotics," *Automatica*, vol. 167, p. 111767, 2024.

[18] S. Liu, P.-Y. Chen, B. Kailkhura, G. Zhang, A. O. Hero III, and P. K. Varshney, "A primer on zeroth-order optimization in signal processing and machine learning: Principals, recent advances, and applications," *IEEE Signal Processing Magazine*, vol. 37, no. 5, pp. 43–54, 2020.

[19] A. D. Flaxman, A. T. Kalai, and H. B. McMahan, "Online convex optimization in the bandit setting: gradient descent without a gradient," *arXiv preprint cs/0408007*, 2004.

[20] X. Chen, Y. Tang, and N. Li, "Improve single-point zeroth-order optimization using high-pass and low-pass filters," in *International Conference on Machine Learning*. PMLR, 2022, pp. 3603–3620.

[21] Y. Nesterov and V. Spokoiny, "Random gradient-free minimization of convex functions," *Foundations of Computational Mathematics*, vol. 17, pp. 527–566, 2017.

[22] J. C. Duchi, M. I. Jordan, M. J. Wainwright, and A. Wibisono, "Optimal rates for zero-order convex optimization: The power of two function evaluations," *IEEE Transactions on Information Theory*, vol. 61, no. 5, pp. 2788–2806, 2015.

[23] A. Agarwal, O. Dekel, and L. Xiao, "Optimal algorithms for online convex optimization with multi-point bandit feedback." in *Colt*, 2010, pp. 28–40.

[24] G. N. Grapiglia, "Worst-case evaluation complexity of a derivative-free quadratic regularization method," *Optimization Letters*, vol. 18, no. 1, pp. 195–213, 2024.

[25] E. Davison, "The robust control of a servomechanism problem for linear time-invariant multivariable systems," *IEEE Transactions on Automatic Control*, vol. 21, no. 1, pp. 25–34, 1976.

[26] H. K. Khalil, *Nonlinear Systems*, 2nd ed. Prentice Hall, 1995.

[27] Z. Jiang and Y. Wang, "Input-to-state stability for discrete-time nonlinear systems," *Automatica*, vol. 37, no. 6, pp. 857–869, 2001.

[28] O. Shamir, "An optimal algorithm for bandit and zero-order convex optimization with two-point feedback," *Journal of Machine Learning Research*, vol. 18, no. 52, pp. 1–11, 2017.

[29] M. Danilova, P. Dvurechensky, A. Gasnikov, E. Gorbunov, S. Guminov, D. Kamzolov, and I. Shibaev, "Recent theoretical advances in non-convex optimization," 2021. [Online]. Available: https://arxiv.org/abs/2012.06188